Desoxyrhapontigenin inhibits RANKL-induced osteoclast formation and prevents inflammation-mediated bone loss

PHUONG THAO TRAN[1], DONG-HWA PARK[2], OKHWA KIM[1], SEUNG-HAE KWON[3], BYUNG-SUN MIN[2] and JEONG-HYUNG LEE[1]

[1]Department of Biochemistry, College of Natural Sciences, Kangwon National University, Chuncheon, Gangwon-Do 24341; [2]College of Pharmacy, Catholic University of Daegu, Hayang, Gyeongbuk 38430; [3]Division of Bio-Imaging, Korea Basic Science Institute Chuncheon Center, Chuncheon, Gangwon-Do 24341, Republic of Korea

Received November 6, 2017; Accepted March 15, 2018

DOI: 10.3892/ijmm.2018.3627

Abstract. Desoxyrhapontigenin (DRG), a stilbene compound from *Rheum undulatum*, has been found to exhibit various pharmacological activities, however, its impact on osteoclast formation has not been investigated. The present study investigated the effect of DRG on receptor activator of nuclear factor-κB ligand (RANKL)-induced osteoclast differentiation in mouse bone marrow macrophages (BMMs) and inflammation-induced bone loss *in vivo*. BMMs or RAW264.7 cells were treated with DRG, followed by an evaluation of cell viability, RANKL-induced osteoclast differentiation, actin-ring formation and resorption pits activity. The effects of DRG on the RANKL-induced phosphorylation of MAPK and the expression of nuclear factor of activated T cells cytoplasmic 1 (NFATc1) and c-Fos were evaluated using western blot analysis once the BMMs were exposed to RANKL and DRG. The expression levels of osteoclast marker genes were also evaluated using western blot analysis and reverse transcription-quantitative polymerase chain reaction A lipopolysaccharide (LPS)-induced murine bone loss model was used to evaluate the protective effect of DRG on inflammation-induced bone-loss. The results demonstrated that DRG suppressed the RANKL-induced differentiation of BMMs into osteoclasts, osteoclast actin-ring formation and bone resorption activity in a dose-dependent manner. Furthermore, DRG significantly inhibited LPS-induced bone loss in a mouse model. At the molecular level, DRG inhibited the RANKL-induced activation of extracellular signal-regulated kinase, the expression of c-Fos, and the induction of NFATc1, a crucial transcription factor for osteoclast formation. DRG decreased the expression levels of osteoclast marker genes, including matrix metalloproteinase-9, tartrate-resistant acid phosphatase and cathepsin K. In conclusion, these findings suggested that DRG inhibited the differentiation of BMMs into mature osteoclasts by suppressing the RANKL-induced activator protein-1 and NFATc1 signaling pathways, and may be a potential candidate for treating and/or preventing osteoclast-associated diseases, including osteoporosis.

Correspondence to: Dr Byung-Sun Min, College of Pharmacy, Catholic University of Daegu, 13-13 Hayang-ro, Hayang, Gyeongbuk 38430, Republic of Korea
E-mail: bsmin@cu.ac.kr

Dr Jeong-Hyung Lee, Department of Biochemistry, College of Natural Sciences, Kangwon National University, 1 Gangwondaehak-gil, Chuncheon, Gangwon-Do 24341, Republic of Korea
E-mail: jhlee36@kangwon.ac.kr

Key words: desoxyrhapontigenin, stilbene, receptor activator of nuclear factor-κB ligand, osteoclastogenesis, bone resorption

Introduction

Bone mass homeostasis is regulated by a delicate balance between osteoclast-mediated bone degradation and osteoblast-induced bone formation, a process termed bone remodeling (1). Osteoclasts are large cells with multiple nuclei, which form from hematopoietic progenitors of the monocyte/macrophage lineage. The cells are specialized in bone resorption (2). Several pathological bone-related diseases, including postmenopausal osteoporosis, rheumatoid arthritis, periodontitis and lytic bone metastasis, are associated with excessive bone breakdown by an increase in the number and activity of osteoclasts (3-5).

Macrophage-colony stimulating factor (M-CSF) and receptor activator of nuclear factor (NF)-κB ligand (RANKL) are two major cytokines, which regulate osteoclast differentiation (6-8). M-CSF is responsible for the proliferation and survival of osteoclast precursors and stimulates the expression of receptor activator of NF-κB (RANK), a receptor for RANKL, with RANKL inducing osteoclast differentiation (7). The binding of RANKL to its receptor, RANK, triggers several downstream signaling pathways, including the p38, extracellular signal-regulated kinase (ERK) and c-Jun N-terminal kinase (JNK) mitogen-activated protein kinase (MAPK) and NF-κB pathways, which lead to the activation of c-Fos and nuclear factor of activated T cells cytoplasmic 1 (NFATc1) (9-14). NFATc1, a master transcription factor of osteoclast formation, induces several genes responsible for osteoclast differentiation and

function, including matrix metalloproteinase-9 (MMP-9), tartrate-resistant acid phosphatase (TRAP) and cathepsin K (CtsK) (15,16).

There are many natural compounds that can be exploited in the development of novel drugs (17). Several compounds from natural products suppress osteoclast formation and function. These products have potential therapeutic value for bone-related diseases characterized by the hyperactivation of osteoclast activity (18). *Rheum undulatum* is a perennial plant that belongs to the Polygonaceae family and is mainly distributed in Korea. The rhizomes of *R. undulatum* and other *Rheum* species, commonly known as rhubarb, have been used for the prevention of a number of diseases in traditional medicines (19,20). Anthraquinones and stilbenes are the primary constituents from the rhizomes of *R. undulatum*. Anthraquinones have a laxative effect (21), whereas the stilbenes from this plant exhibit various pharmacological activities, which include antioxidant, anti-inflammatory and hepatoprotective effects (22,23). Desoxyrhapontigenin (DRG) is a stilbene compound isolated from the rhizomes of *R. undulatum* and has an anti-inflammatory effect via activating the nuclear factor erythroid 2-related factor 2/heme oxygenase-1 pathway and attenuating the NF-κB and MAPK pathways in macrophages (24). However, the anti-osteoclastogenic effect of DRG and its underlying mechanisms remain to be fully elucidated. On the basis of the association between chronic inflammatory and bone diseases (25), the present study aimed to determine the pharmacological effects of DRG on RANKL-induced osteoclast formation and function in mouse bone marrow macrophages (BMMs) and on bone loss induced by lipopolysaccharide (LPS) in an *in vivo* animal model. It was demonstrated that DRG suppressed RANKL-induced osteoclast formation at an early stage of osteoclastogenesis in BMMs and prevented LPS-induced bone destruction in the animal model.

Materials and methods

Isolation of stilbene derivatives. Dried *R. undulatum* L. rhizomes were purchased from the Yakryoung-si folk medicine market in Daegu, Korea, in May 2015. Botanical identification was performed by Professor Byung-Sun Min (College of Pharmacy, Catholic University of Daegu, Hayang, Korea). A voucher specimen (CUD-1188-1) was stored at the College herbarium. The MeOH extract of the dried rhizomes of *R. undulatum* L. was concentrated to yield a residue (4.5 kg), which was suspended in water and then successively partitioned with *n*-hexane, ethyl acetate and *n*-butanol to afford *n*-hexane-, EtOAc-, and *n*-BuOH-soluble fractions, and a water (H_2O) layer. The EtOAc-soluble fraction (658 g) was subjected to silica gel column chromatography and eluted with *n*-hexane-EtOAc (7:1→0:1) to yield six fractions (E1-E6). Fraction E2 was rechromatographed on a silica gel column eluted with chloroform ($CHCl_3$)-MeOH (7:1→0:1) to yield six sub-fractions (E2-1-E2-6). Subsequently, the E2-1 sub-fraction was chromatographed on an RP-18 silica gel column with MeOH-H_2O (1:1→1:0) as the mobile phase to yield five fractions (E2-1-1-E2-1-5). Sub-fraction E2-1-3 was subjected to silica gel column chromatography using a stepwise gradient elution of $CHCl_3$-MeOH (14:1→0:1), to yield rhapontigenin (2.1 g) and resveratrol (200 mg). Sub-fraction E2-1-4 was rechromatographed on a silica gel column with CH_2Cl_2-MeOH-H_2O (5:1:1) to obtain DRG (500 mg). Fraction E3 was fractionated on a silica gel column using $CHCl_3$-MeOH (20:1→0:1) as the solvent system to obtain piceatannol (3 g). Sub-fraction E3-3 was purified using high-performance liquid chromatography with a stepwise gradient of H_2O-MeOH (1:1→3:1) to yield resveratroloside (15 mg). The structures of the stilbene derivatives are shown in Fig. 1. The purity of these stilbenes was assessed using ^1H and ^{13}C nuclear magnetic resonance spectra. The spectra revealed signals with a high level of purity with no impurities.

Cell culture. RAW264.7 cells were obtained from the American Type Culture Collection (Manassas, VA, USA) and were cultured in Dulbecco's modified essential medium with 10% heat-inactivated fetal bovine serum (FBS; Cambrex, Charles City, IA, USA) and penicillin (100 U/ml)-streptomycin (100 µg/ml). The cells were cultured at 37˚C in a humidified 5% CO_2 atmosphere.

Isolation of BMMs and osteoclast differentiation. Bone marrow cells were isolated from the femurs and tibias of 6-week-old male ICR mice weighing 22-25 g (DBL, Emseong, Chungbuk, Korea) housed at a temperature of 24±2˚C and humidity of 55±10% controlled colony room under a 12 h light and 12 h dark cycle. All mice were allowed *ad libitum* access to a standard chow diet and water prior to all experiments. The bone marrow cells were then cultured in α-MEM (HyClone; GE Healthcare Life Sciences, Logan, UT, USA) containing 10% FBS, 100 U/ml penicillin, 100 µg/ml streptomycin and 10 ng/ml M-CSF (Prospec-Tany TechnoGene Ltd., East Brunswick, NJ, USA) overnight in a humidified incubator with 5% CO_2 at 37˚C. The floating cells were harvested and maintained for 3 days with 30 ng/ml M-CSF. The cells adhered to the culture dish were characterized as BMMs and used for subsequent experiments. The BMMs ($5x10^4$ cells/well) were cultured in 96-well plates and maintained with RANKL (100 ng/ml) and M-CSF (30 ng/ml) for 7 days in the presence or absence of the indicated compounds. The medium was replaced every 2 days. The cells were then fixed for 15 min in 3.7% formalin, permeabilized with 0.1% Triton X-100, and stained for TRAP with an acid phosphatase leukocyte kit (Sigma-Aldrich; EMD Millipore, Billerica, MA, USA). TRAP-positive multinucleated cells with more than five nuclei were defined as osteoclasts.

Antibodies and reagents. Recombinant mouse RANKL and M-CSF were obtained from R&D Systems, Inc. (Minneapolis, MN, USA). Antibodies targeting NFATc1 (cat no. 8032S), c-Fos (cat no. 2250S), c-Src (cat no. 2019), ERK1/2 (cat no. 4695S), p38 (cat no. 9212), JNK (cat no. 9252), phospho-p38 (cat no. 9216S), phospho-ERK1/2 (cat no. 9101S) and phospho-JNK (cat no. 4668S) were purchased from Cell Signaling Technology, Inc. (Danvers, MA, USA). Fluorescein isothiocyanate (FITC)-conjugated palloidin (cat no. A12379) was from Invitrogen; Thermo Fisher Scientific, Inc. (Waltham, MA, USA). Antibodies targeting α-tubulin (cat no. SC-5546) and CtsK (cat no. SC48353) were obtained from Santa Cruz Biotechnology, Inc. (Santa Cruz, CA, USA).

A

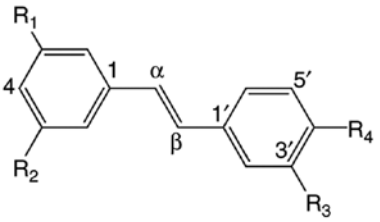

	R1	R2	R3	R4
Desoxyrhapontigenin (1)	OH	OH	H	OMe
Rhapontigenin (2)	OH	OH	OH	OMe
Resveratrol (3)	OH	OH	H	OH
Piceatannol (4)	OH	OH	OH	OH
Resveratroloside (5)	OH	OH	H	OGlu

B

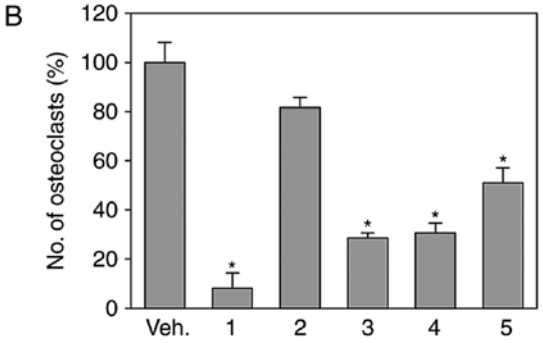

Figure 1. Chemical structures of the isolated stilbenes from *R. undulatum* and their effects on RANKL-induced osteoclast formation in BMMs. (A) Chemical structures of the isolated stilbenes. (B) Effect of the five isolated stilbenes on the RANKL-induced differentiation of BMMs into osteoclasts. BMMs were induced to differentiate into osteoclasts by incubating with macrophage-colony stimulating factor (30 ng/ml) and RANKL (100 ng/ml) in the presence or absence of the indicated stilbenes (10 μM) for 7 days, and then a TRAP assay was performed. The quantities of TRAP-positive multinucleated (>5 nuclei) osteoclasts were determined following image capture (magnification, x40). Data are presented as the mean ± standard error of the mean (*P<0.01, compared with Veh; n=3). BMMs, bone marrow macrophages; RANKL, receptor activator of nuclear factor-κB ligand; TRAP, tartrate-resistant acid phosphatase; Veh, vehicle-treated control.

Cytotoxicity assay. Cytotoxicity was measured using a 3-(4,5-dimethylthiazol-2-yl)-2,5-diphenyl tetrazolium bromide (MTT)-based assay. The BMMs were cultured into 96-well plates (1x10^4 cells/well) and supplemented with 30 ng/ml M-CSF in the presence of the indicated concentrations of DRG. After 72 h, 0.5 mg/ml of MTT was added to each well for 3 h. At the end of the incubation, the insoluble formazan products were dissolved in dimethyl sulfoxide, and absorbance at 540 nm was determined.

Bone resorption assay. The BMMs (5x10^4 cells/well) were seeded in OsteoAssay Surface 96-well plates (Corning Incorporated, Corning, NY, USA) in α-MEM supplemented with 10% FBS, 1% penicillin and streptomycin, 30 ng/ml M-CSF, 100 ng/ml RANKL, and various concentrations of DRG. The culture medium was replaced every 2 days and culture continued for 7 days. The differentiated BMMs were washed with tap water and images of the surface of resorption pits were captured using a model H550L microscope (Nikon Corporation, Tokyo, Japan) and quantified via ImageJ software [Java 1.6.0_20 (64-bit); NIH, Bethesda, MD, USA].

Actin ring formation and immunofluorescence. The BMMs (10^6 cells/ml) were seeded on a cover glass and cultured for 7 days with 30 ng/ml M-CSF and 100 ng/ml RANKL in the presence of the indicated concentrations of DRG. The BMMs were washed and fixed in 15 min with 4% paraformaldehyde. Following permeabilization with 0.1% Triton X-100, the BMMs were stained for 10 min with FITC-phalloidin at room temperature. Following washing with phosphate buffered saline (PBS), the BMMs were mounted and images were captured using an LSM510 META NLO inverted confocal laser scanning microscope (Zeiss GmbH, Jena, Germany; Korea Basic Science Institute Chuncheon Center, Chuncheon, Korea) equipped with an external Argon, HeNe laser and HeNe laser II.

Western blot analysis. The cells were harvested and lysed in a lysis buffer containing 150 mM NaCl, 50 mM Tris-HCl (pH 7.4), 1 mM EDTA, 1% NP-40, 5 mM sodium orthovanadate and protease inhibitor cocktail (BD Biosciences, Franklin Lakes, NJ, USA), and then centrifuged for 10 min at 4˚C and 22,000 x g. Protein concentration was determined using the Bradford method (26). A total of 30 μg of cellular extracts was separated via 8% sodium dodecyl sulfate-polyacrylamide gel electrophoresis and then transferred onto a Hybond-P membrane (GE Healthcare Life Sciences, Chalfont, UK). The membranes were blocked with 5% nonfat skim milk at room temperature for 1 h and probed for 2 h with the indicated primary antibodies (1:1,000 dilution). Following washing with PBS containing 0.1% Tween-20, the membranes were incubated with the secondary antibody (1:2,000 dilution) at room temperature for 2 h. The signal was detected using the enhanced chemiluminescence system (Thermo Fisher Scientific, Inc.).

Reverse transcription-quantitative polymerase chain reaction (RT-qPCR) analysis. The BMMs were collected and total RNA was extracted using an RNeasy Mini kits according to the manufacturer's protocol (Qiagen, Inc., Valencia, CA, USA). The first-strand cDNA was synthesized using 1 μg of total RNA. RT-qPCR analysis was performed using TOPreal qPCR 2X PreMIX (SYBR-Green; Enzynomics, Inc., Daejon, Korea) and the Rotor-Gene Q real-time PCR cycler (Qiagen, Inc.). The primers sequence were as follows: MMP-9, forward, 5'-TGG GCAAGCAGTACTCTTCC-3' and reverse, 5'-AACAGGCTG TACCCTTGGTC-3'; CtsK, forward, 5'-GACACCCAGTGG GAGCTATG-3' and reverse, 5'-AGAGGCCTCCAGGTTATG GG-3'; TRAP, forward, 5'-ACTTGCGACCATTGTTAGCC-3' and reverse, 5'-TTCGTTGATGTCGCACAGAG-3'; β-actin, forward, 5'-GGGAAATCGTGCGTGACATCAAAG-3' and reverse, 5'-AACCGCTCCTTGCCAATAGT-3'. The PCR conditions were as follows: 95˚C for 10 min, followed by 40 cycles at 95˚C for 10 sec, 60˚C for 15 sec and 72˚C for 20 sec. All reactions were performed in triplicate and β-actin was used as an internal control. Quantification of the relative gene expression was computed using the $2^{-\Delta\Delta Cq}$ method (27).

LPS-induced bone loss in vivo. All experimental protocols were approved by the Institutional Animal Care and Use

Committee (IACUC) of Kangwon National University (IACUC approval No. KW-180119-3). To investigate the effect of DRG on inflammation-induced bone loss, the mice were randomly divided into control vehicle-treated, LPS-treated, DRG-treated, and DRG + LPS-treated groups (n=4/group). The mice in the control group were treated with control vehicle (dimethyl sulfoxide: cremophor-EL in PBS; 1:1:8). The mice were injected intraperitoneally with DRG (50 mg/kg) solubilized in dimethyl sulfoxide: Chremophore-EL in PBS (1:1:8 by volume) or control vehicle for 1 h prior to the first LPS (5 mg/kg) injection and then every other day for 8 days. LPS was injected on days 2 and 6. All mice were sacrificed on day 9. Intact left femoral metaphysic regions of each mouse were evaluated by high-resolution micro-computed tomography (micro-CT) analysis using an NFR-Polaris-S160 apparatus (Nanofocus Ray; Korea Basic Science Institute Chuncheon Center) with a 90 μA current, source voltage of 45 kVp and 7 μm isotropic resolution. Femoral scans were performed over 2 mm from the growth plate, with a total of 350 sections per scan. Following three-dimensional (3D) reconstruction, trabecular number (Tb.N), bone volume per tissue volume (BV/TV), trabecular separation (Tb.Sp) and bone surface/bone volume (BS/BV) were examined with quantitative analyses using INFINITT-Xelis software (version 1.7; INFINITT Healthcare Co., Ltd., Seoul, Korea).

Statistical analysis. Data are presented as the mean ± standard error of the mean. Statistical analysis was performed using SPSS (version 14.0; SPSS Inc., Chicago, IL, USA). Statistical significance was assessed by one-way analysis of variance and the difference between the experimental groups was compared. $P<0.05$ was considered to indicate a statistically significant difference.

Results

Isolation of the stilbene derivatives from R. undulatum and their anti-osteoclastogenic effects in BMMs. In order to identify novel anti-osteoclastogenic compounds from the natural products, the stilbene derivatives were isolated from *R. undulatum*. Repeated column chromatography of the $CHCl_3$-soluble fraction of *R. undulatum* on a silica gel and RP-C_{18} led to the isolation of five stilbenes. These stilbenes were identified as DRG, rhapontigenin, resveratrol, piceatannol and resveratroloside, by comparison with the published spectroscopic data (28-30). Their structures are shown in Fig. 1A. To investigate the effects of these stilbenes on osteoclast formation, the effects of these stilbenes on RANKL-induced osteoclast formation were investigated in mouse BMMs. At 10 μM, DRG, resveratrol, piceatannol and resveratroloside significantly reduced the RANKL-induced formation of osteoclasts as characterized by TRAP-positive multinucleated cells. However, rhapontigenin did not significantly inhibit osteoclast formation (Fig. 1B). As resveratrol and piceatannol are reported to have anti-osteoclastogenic activities (31,32) and DRG exhibited potent anti-osteoclastogenic activity, the present study further investigated the anti-osteoclastogenic effect of DRG.

DRG inhibits RANKL-induced formation in mouse BMMs and RAW264.7 cells. To investigate the effects of DRG on RANKL-induced osteoclast formation in detail, the anti-osteoclastogenic activity of DRG was evaluated using mouse BMMs and RAW264.7 cells. The mouse BMMs were incubated with RANKL and M-CSF for 7 days, and the RAW264.7 cells were stimulated with RANKL for 4 days. Treating BMMs or RAW264.7 cells with DRG reduced the formation of osteoclasts in a dose-dependent manner, as measured by TRAP-positive multinucleated cells (Fig. 2A and B). Subsequently, whether DRG down-regulated the RANKL-induced expression of osteoclast markers, including c-Src and CtsK, in the BMMs was evaluated. Western blot analysis revealed that DRG effectively suppressed the RANKL-induced upregulation of these markers (Fig. 2C), suggesting that DRG suppressed RANKL-induced osteoclast formation. To investigate whether DRG inhibited RANK-induced osteoclastogenesis due to the potential cytotoxicity of DRG to BMMs, the cytotoxic effect of DRG on BMMs was examined. The MTT assay results showed that DRG was not cytotoxic towards BMMs up to 30 μM (Fig. 2D). These results suggested that DRG suppressed RANKL-induced osteoclastogenesis without affecting the viability of BMMs.

To determine whether DRG inhibits the early or late stage of osteoclast formation, the present study investigated the effects of DRG on RANKL-induced osteoclast precursor differentiation by treating at different times between days 1 and 5 post-RANKL stimulation (Fig. 2E). DRG significantly reduced RANKL-induced osteoclast formation at day 1 of treatment. However, DRG was not effective in the suppression of osteoclast formation at day 5 of treatment, suggesting that DRG suppresses RANKL-induced osteoclastogenesis at an early stage.

DRG inhibits actin-ring formation and bone resorption in RANKL-stimulated BMMs. To further investigate the effect of DRG on osteoclast differentiation, the present study determined whether DRG inhibited F-actin ring formation, which is a critical indicator of the bone resorption activity of osteoclasts and is a characteristic feature of mature osteoclasts (33). Under the stimulation of RANKL, BMMs formed the F-actin ring structures, as evidenced by FITC-phalloidin staining (Fig. 3A). Treating the BMMs with DRG significantly decreased the number and size of actin-ring structures in a concentration-dependent manner, suggesting that DRG inhibited the formation of mature osteoclasts. To confirm whether DRG suppressed the bone-resorbing activity of osteoclasts, the effect of DRG on RANKL-induced bone resorption in BMMs was investigated (Fig. 3B). In the presence of RANKL, osteoclasts formed bone-resorption pits. However, DRG markedly reduced the formation of pits formed in the overall osteoassay surface in a concentration-dependent manner. These results demonstrated that DRG suppressed RANKL-induced bone resorption ability.

DRG suppresses LPS-induced bone loss in vivo. The involvement of DRG in the inhibition of osteoclastogenesis *in vivo* was assessed using an inflammation-induced bone loss mouse model. The mice were treated with LPS in the presence or absence of DRG. After 9 days, the femurs were examined by micro-CT. 3D analysis revealed that LPS administration appeared to cause trabecular bone loss in the femurs.

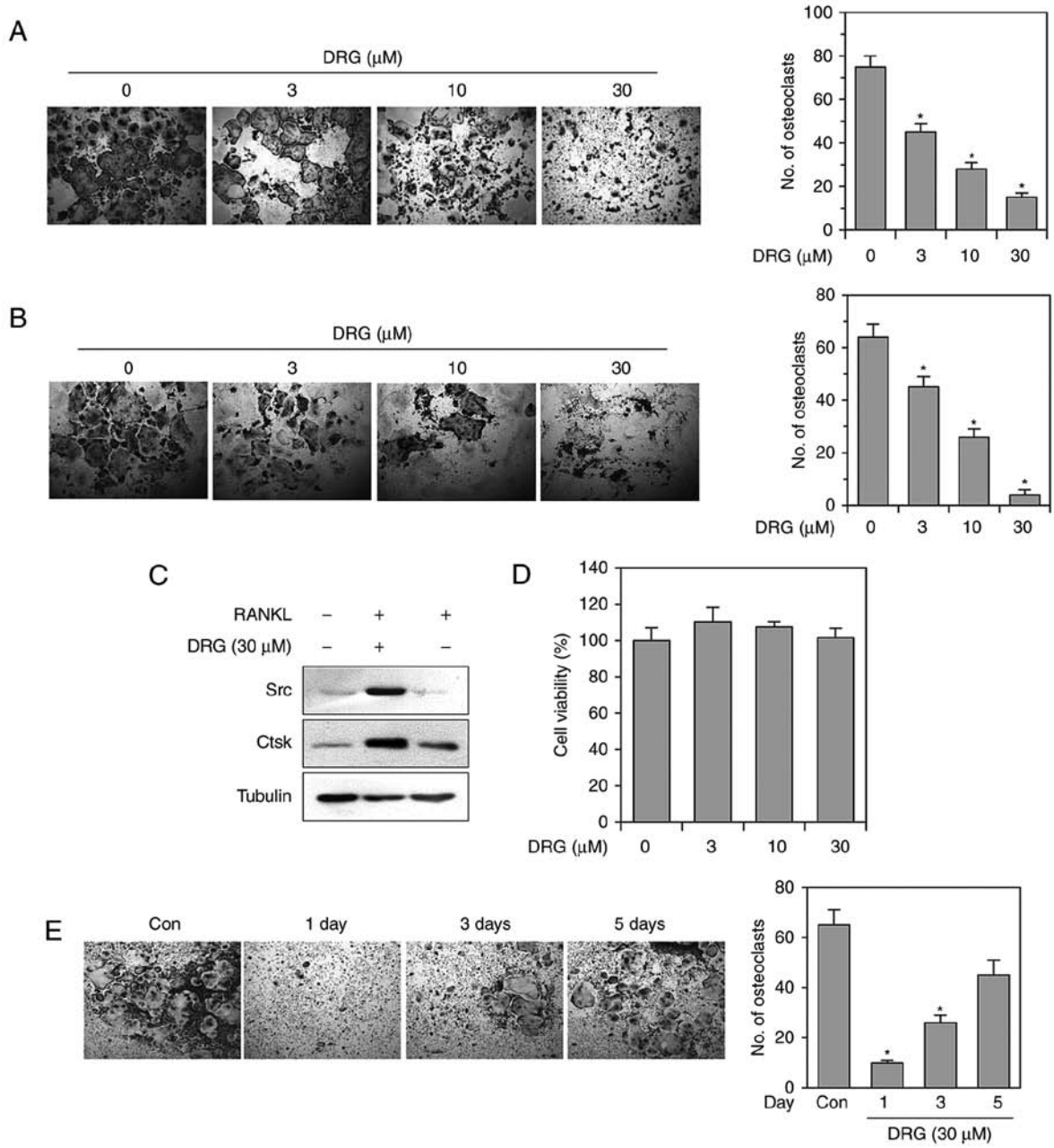

Figure 2. DRG inhibits RANKL-induced osteoclast formation at the early stage. (A) BMMs were induced to differentiate into osteoclasts by incubating with M-CSF (30 ng/ml) and RANKL (100 ng/ml) in the presence or absence of the indicated concentrations of DRG for 7 days, and then a TRAP assay was performed. The quantities of TRAP-positive multinucleated (>5 nuclei) osteoclasts were determined following image capture (magnification, x40). Data are presented as the mean ± standard error of the mean (*P<0.01, compared with vehicle-treated control; n=3). (B) RAW264.7 cells were induced to differentiate into osteoclasts by incubating with RANKL (100 ng/ml) in the presence or absent of the indicated concentrations of DRG for 4 days, and then a TRAP assay was performed. The quantities of TRAP-positive multinucleated (>5 nuclei) osteoclasts were determined following image capture (magnification, x40). Data are presented as the mean ± standard error of the mean (*P<0.01, compared with vehicle-treated control; n=3). (C) BMMs were stimulated with M-CSF (30 ng/ml) and RANKL (100 ng/ml), in the presence or absence of DRG (30 μM) for 7 days. Total lysates were prepared and the expression levels of c-Src and cathepsin K were determined by western blot analysis. (D) BMMs were seeded into 96-well plates with M-CSF (30 ng/ml), followed by incubation with the indicated concentrations of DRG for 3 days. Cell viability was measured using the MTT assay. Data are presented as mean ± standard error of the mean (*P<0.01, compared with vehicle-treated control; n=3). (E) Effect of DRG on RANKL-induced osteoclast formation at different time points. BMMs were induced to differentiate into osteoclasts by incubating with M-CSF (30 ng/ml) and RANKL (100 ng/ml), and then treated with 30 μM DRG at the indicated periods of time. The cells were cultured for 7 days, and then fixed and the TRAP staining assay was performed. The quantities of TRAP-positive multinucleated (>5 nuclei) osteoclasts were determined following image capture (magnification, x40). Data are presented as the mean ± standard error of the mean (*P<0.01, compared with Con; n=3). BMMs, bone marrow macrophages; DRG, desoxyrhapontigenin; RANKL, receptor activator of nuclear factor-κB ligand; TRAP, tartrate-resistant acid phosphatase; Con, control; M-CSF, macrophage-colony stimulating factor.

However, LPS-induced bone loss was considerably reduced in mice who received DRG (Fig. 4A). In correlation with micro-CT images, the reductions of Tb. N and BV/TV by LPS injection were rescued in DRG-treated mice (Fig. 4B). The LPS-induced changes in Tb.Sp and BS/BV were also attenuated by DRG administration (Fig. 4B). These results indicated that DRG suppressed inflammation-induced osteoclast formation *in vivo*.

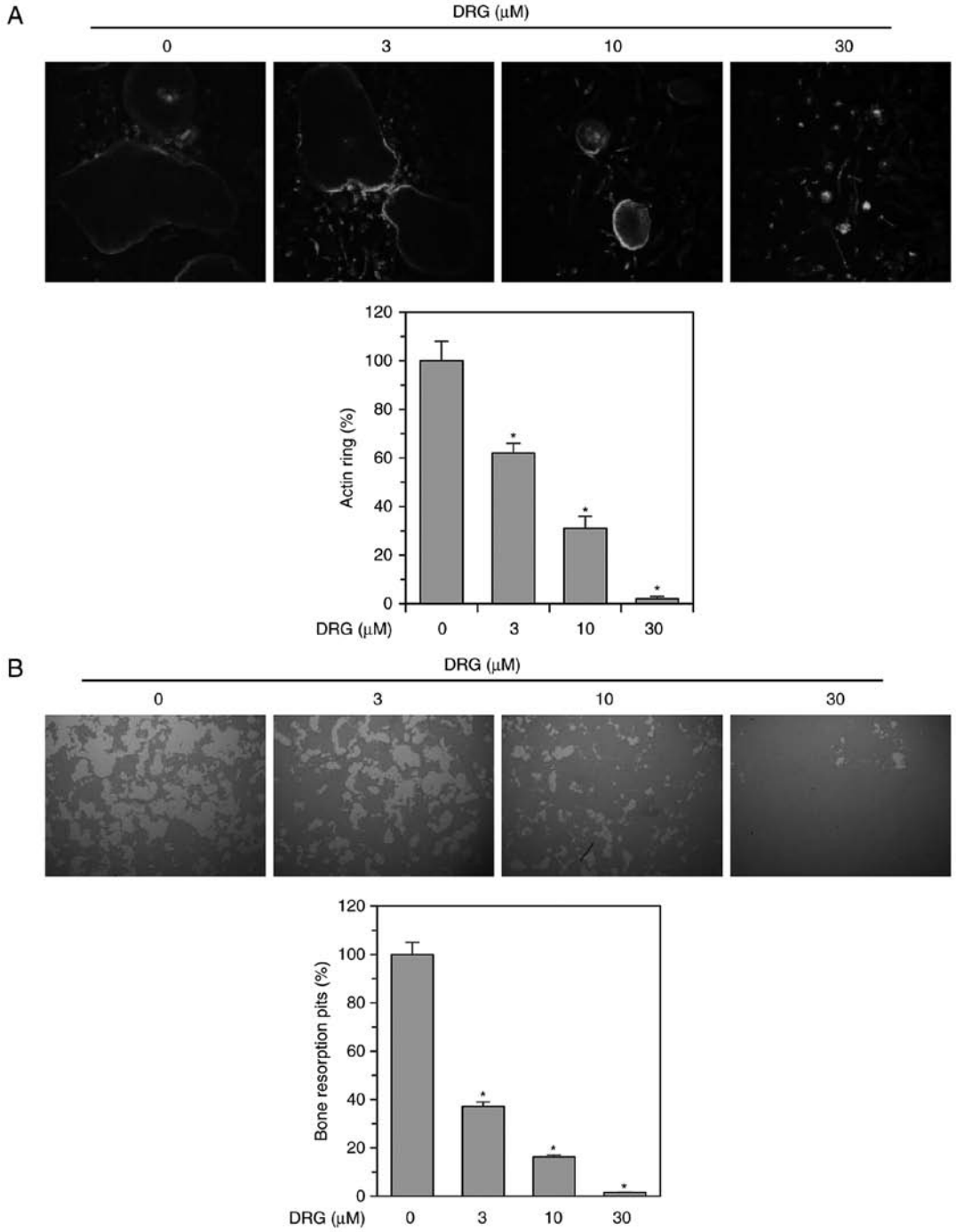

Figure 3. DRG suppresses RANKL-induced actin-ring formation and resorption pits in BMMs. (A) BMMs were induced to differentiate into osteoclasts by incubating with M-CSF (30 ng/ml) and RANKL (100 ng/ml) in the presence or absence of the indicated concentrations of DRG for 7 days. Actin-ring positive osteoclasts were visualized with fluorescein isothiocyanate-conjugated phalloidin. Data are presented as the mean ± standard error of the mean (*P<0.01, compared with vehicle-treated control; n=3). (B) BMMs were seeded on Corning OsteoAssay Surface 24-well plates and incubated with RANKL (100 ng/ml) and M-CSF (30 ng/ml) in the presence of various concentrations of DRG for 6 days. The cells were washed and pit areas were analyzed with ImageJ software. Data are presented as the mean ± standard error of the mean (*P<0.01, compared with vehicle-treated control; n=3). BMMs, bone marrow macrophages; DRG, desoxyrhapontigenin; RANKL, receptor activator of nuclear factor-κB ligand; M-CSF, macrophage-colony stimulating factor.

DRG inhibits the RANKL-induced activation of ERK, c-Fos and NFATc1. The finding that DRG suppressed RANKL-induced osteoclast formation at an early stage prompted an experiment designed to examine the effect of DRG on RANKL-induced early signaling events, including MAPK pathways. BMMs showed increased phosphorylation levels of ERK, p38 and JNK MAPKs in the BMMs upon stimulation with RANKL. Pretreatment with DRG did not decrease the phosphorylation levels of p38 and JNK. However, DRG suppressed the RANKL-induced phosphorylation of ERK (Fig. 5A). Activation of MAPK signaling pathways induces the expression of NFATc1 via activator protein-1 (AP-1) transcription factor (14), which is a heterodimer of the c-Jun and c-Fos transcription factors. Therefore, the present study determined whether DRG suppresses the RANKL-induced expression of c-Fos and NFATc1. Stimulation of the BMMs

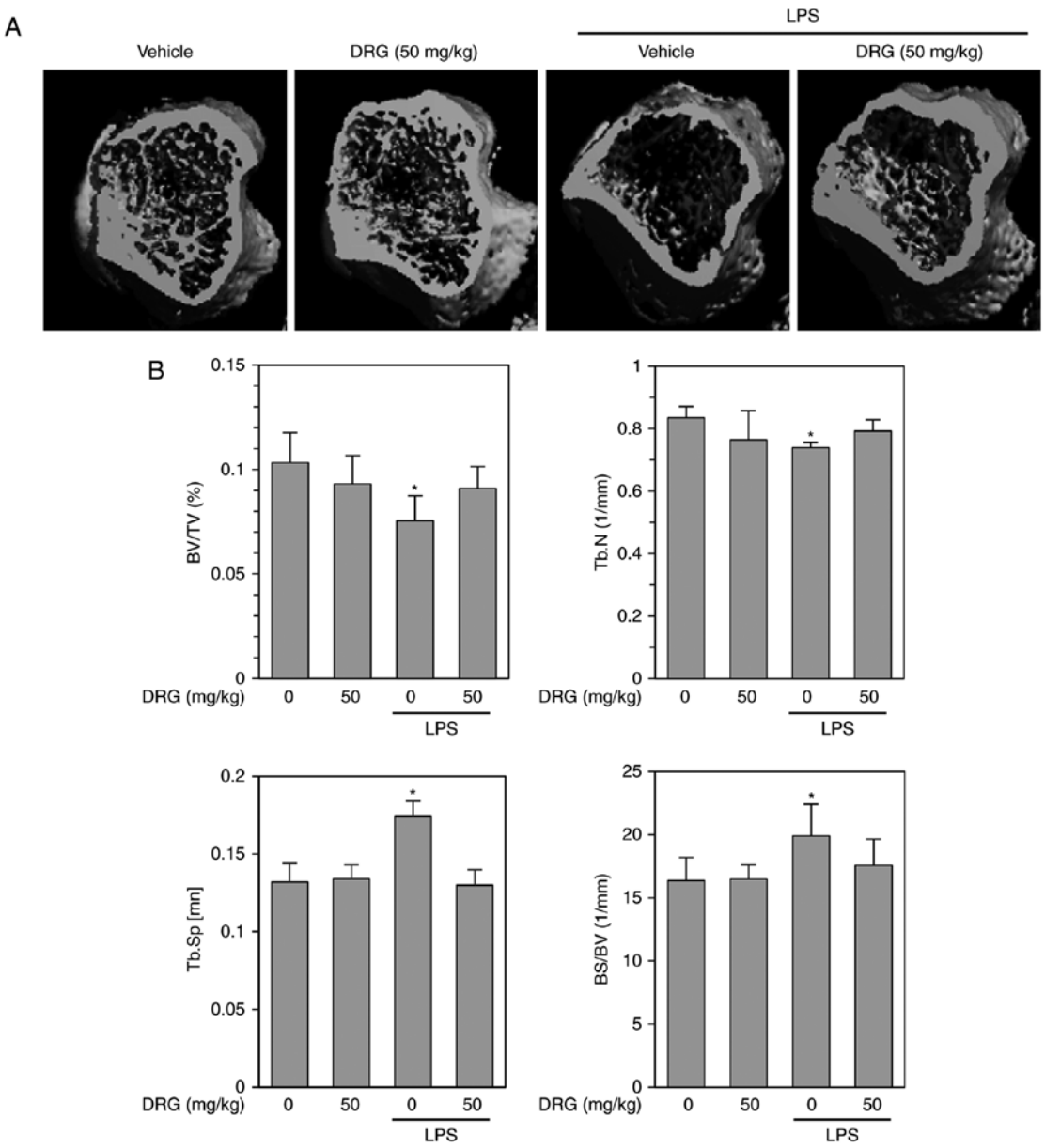

Figure 4. DRG suppresses LPS-induced bone loss *in vivo*. (A) At 9 days following the first LPS injection, mice were sacrificed, their femurs were collected and their three-dimensional images were generated using micro-computed tomography. (B) BV/TV, Tb. N, Tb. Sp, and BS/BV were obtained using the CTAn software. n=4 (eight legs) in each group. *P<0.05, compared with vehicle-treated control. DRG, desoxyrhapontigenin; LPS, lipopolysaccharide; BV/TV, bone volume per tissue volume; Tb. N, trabecular number; Tb. Sp, trabecular separation; BS/BV, bone surface to bone volume.

with RANKL increased the expression levels of c-Fos and NFATc1. However, the RANKL-induced expression of c-Fos and NFATc1 was attenuated by DRG treatment (Fig. 5B), suggesting that DRG suppressed RANKL-induced osteoclastogenesis, at least in part by inhibiting the MAPK/AP-1 signaling pathway.

DRG inhibits the expression of NFATc1 target genes. To further examine the role of DRG in the activation of NFATc1, the present study examined the effects of DRG on the expression of marker genes associated with osteoclastogenesis, including CtsK, MMP-9 and TRAP. These three genes are downstream target genes of the NFATc1 pathway. DRG significantly inhibited the expression of these NFATc1 target genes in a time- and concentration-dependent manner during RANKL-induced osteoclastogenesis (Fig. 6).

Discussion

Osteoclasts are specialized multinucleated cells, which are able to resorb the collagen matrix of bone. An aberrant increase in RANKL/RANK signaling results in increased osteoclast formation and activity, as reported in various bone loss-related diseases, including postmenopausal osteoporosis, autoimmune arthritis, bone tumors and periodontitis. Therefore, the inhibition of osteoclast differentiation and/or its function may be a potential approach to treat or prevent pathological bone loss. To this end, attention has turned to stilbenes. Stilbenes are a class of plant polyphenols and, due to the potential in therapeutic applications, their derivatives are promising for drug research and development (34). Resveratrol, a naturally occurring stilbene, and/or a variety of plant food containing resveratrol has a therapeutic potential for treatment or prevention of age-related

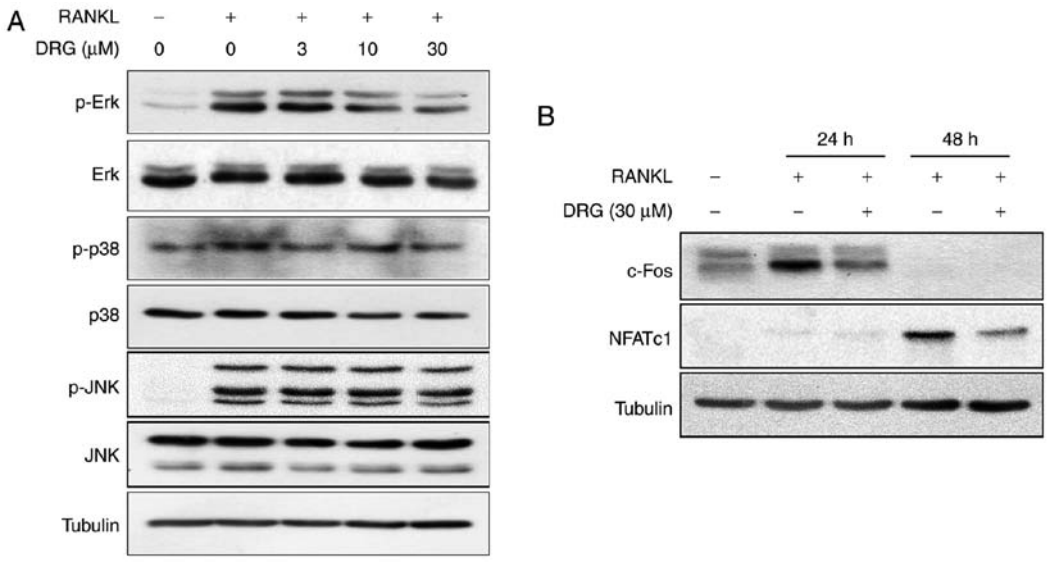

Figure 5. DRG inhibits RANKL-induced ERK phosphorylation in BMMs. (A) BMMs were stimulated with RANKL (100 ng/ml) for 10 min in the presence of the indicated concentrations of DRG. Western blot analysis was performed to determine the expression levels of p-ERK, p-JNK and p-p38. (B) BMMs were stimulated with RANKL (100 ng/ml) for the indicated periods of time in the presence or absence of 30 μM DRG. Western blot analysis was performed to determine the expression levels of c-Fos and NFATc1. BMMs, bone marrow macrophages; DRG, desoxyrhapontigenin; RANKL, receptor activator of nuclear factor-κB ligand; ERK, extracellular signal regulated kinase; JNK, c-Jun N-terminal kinase; p-, phosphorylated; NFATc1, nuclear factor of activated T cells cytoplasmic 1.

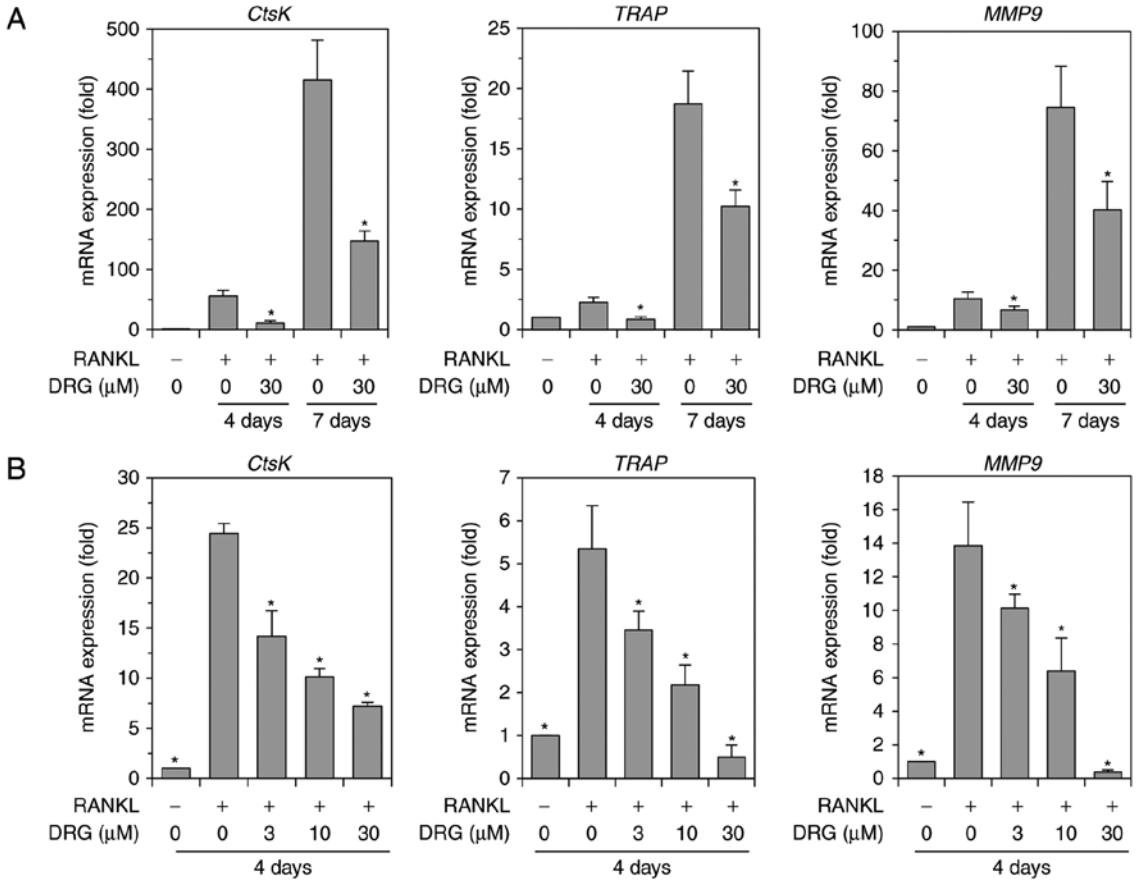

Figure 6. DRG impairs the RANKL-induced expression of NFATc1 target genes. (A) BMMs were incubated with RANKL (100 ng/ml) in the presence or absence of 30 μM DRG for the indicated periods of time. RT-qPCR analysis was performed to quantify the mRNA expression levels of CtsK, TRAP and MMP-9. Data are presented as the mean ± standard error of the mean (*P<0.01, compared with the RANKL-only treated control; n=5). (B) BMMs were pretreated with the indicated concentration of DRG under the stimulation of RANKL (100 ng/ml) for 4 days. RT-qPCR analysis was performed to quantify the mRNA expression levels of CtsK, TRAP and MMP-9. Data are presented as the mean ± standard error of the mean (*P<0.01, compared with the RANKL-only treated control; n=5). BMMs, bone marrow macrophages; DRG, desoxyrhapontigenin; RANKL, receptor activator of nuclear factor-κB ligand; TRAP, tartrate-resistant acid phosphatase; CtsK, cathepsin K; MMP-9, matrix metalloproteinase-9; RT-qPCR, reverse transcription-quantitative polymerase chain reaction.

degenerative diseases such as osteoporosis (35,36). DRG is a stilbene isolated from *R. undulatum* and has the anti-inflammatory activity (24). However, the effect of DRG on osteoclast differentiation and its underlying molecular mechanism(s) in osteoclastogeneis remain to be elucidated. In the present study, it was demonstrated that DRG suppressed RANKL-induced osteoclastogenesis at the early stages, but had no cytotoxic effect on BMMs. DRG also prevented inflammation-induced bone destruction in the *in vivo* model. At the molecular level, DRG suppressed the RANKL-induced activation of ERK and NFATc1, and the expression of NFATc1 target genes, including TRAP, CtsK and c-Src. These collective findings support the therapeutic potential of DRG for bone resorption-associated diseases.

M-CSF regulates the proliferation and survival of BMMs, and the differentiation of BMMs to the osteoclast precursor, whereas the differentiation of osteoclast precursors to mature osteoclasts is regulated by RANKL (9). In the present study, it was demonstrated that DRG did not show cytotoxic activity towards the M-CSF-stimulated BMMs. However, DRG did inhibit the RANKL-induced formation of mature osteoclasts from osteoclast precursors, suggesting that DRG suppressed RANKL-induced osteoclastogenesis at the early stage by modulating the RANKL/RANK signaling pathway.

The ERK, JNK, and p38 MAPK pathways are involved in the RANKL/RANK signaling pathway and are important in osteoclastogenesis through their regulation of the expression of NFATc1 via AP-1 transcription factors (9,37). Treating BMMs with JNK- or p38-specific inhibitors suppresses RANKL-induced osteoclast differentiation (38,39). Activation of the ERK signaling pathway is also important for RANKL-induced osteoclastogenesis. Treatment with PD98059, an ERK inhibitor, attenuates osteoclast differentiation (40). In the present study, DRG suppressed the RANKL-induced phosphorylation of ERK and c-Fos, and the expression of NFATc1, suggesting that DRG suppressed RANKL-induced osteoclast differentiation via inhibiting the MAPK/AP-1 signaling pathway.

The present study demonstrated the protective effect of DRG on LPS-induced bone loss *in vivo*. The administration of DRG at 50 mg/kg suppressed LPS-induced bone loss in a mouse model, as conformed by micro-CT analysis, suggesting that DRG may be effective in treating or preventing inflammation-induced bone loss *in vivo* by suppressing osteoclast formation. *R. undulatum* is a rich source of stilbenes, including DRG and resveratrol. DRG is a major constituent of *R. undulatum* (28), and the content of DRG in ethanol extract from the dried rhizomes of *R. undulatum* is ~0.1% (28). The findings in the present study suggested that DRG may be considered as a novel lead compound for the development of a therapeutic or preventive agent against inflammation-induced bone loss. In addition, the DRG-enriched extracts from the rhizomes of *R. undulatum* may be applied as a supplemental or functional food, having a beneficial effect on inflammation-induced bone.

In conclusion, DRG, a stilbene compound, can suppress RANKL-induced osteoclast differentiation in BMMs and LPS-induced bone destruction in an *in vivo* model. DRG impaired the RANKL-induced activation of NFATc1 via the MAPK/AP-1 signaling pathway. These findings indicated that DRG may be a valuable stilbene compound for the prevention and/or treatment of osteoclast-associated bone diseases, including rheumatoid arthritis and osteoporosis.

Acknowledgements

The authors would like to thank Mr. Kim Song-Rae (Korea Basic Science Institute, Chuncheon Center, Chuncheon, Gangwon-Do, Republic of Korea) for technical assistance.

Funding

This study was supported by grants from the National Research Foundation of Korea (grant nos. NRF-2015R1A2A1A15055521 and NRF-2015M3A9A5031271) and the Kangwon National University (2017 Research Grant).

Availability of data and materials

The datasets used and/or analyzed during the current study are available from the corresponding author on reasonable request.

Authors' contributions

PTT performed the experiments and analysed the data. DHP isolated the compounds used in the present study. OK and SHK performed the *in vivo* study. BSM wrote in part and finalized the manuscript. JHL conceptualized and designed the study and finalized the manuscript.

Ethics approval and consent to participate

All experimental protocols were approved by the Institutional Animal Care and Use Committee (IACUC) of Kangwon National University (IACUC approval no. KW-180119-3).

Consent for publication

Not applicable.

Competing interests

The authors declare that they have no competing interests.

References

1. Robling AG, Castillo AB and Turner CH: Biomechanical and molecular regulation of bone remodeling. Annu Rev Biomed Eng 8: 455-498, 2006.
2. Boyce BF, Rosenberg E, de Papp AE and Duong LT: The osteoclast, bone remodelling and treatment of metabolic bone disease. Eur J Clin Invest 42: 1332-1341, 2012.
3. Feng X and McDonald JM: Disorders of bone remodeling. Annu Rev Pathol 6: 121-145, 2011.
4. Hienz SA, Paliwal S and Ivanovski S: Mechanisms of bone resorption in periodontitis. J Immunol Res 2015: 615486, 2015.
5. Crockett JC, Rogers MJ, Coxon FP, Hocking LJ and Helfrich MHL: Bone remodelling at a glance. J Cell Sci 124: 991-998, 2011.
6. Bonewald LF: The amazing osteocyte. J Bone Miner Res 26: 229-238, 2011.
7. Asagiri M and Takayanagi H: The molecular understanding of osteoclast differentiation. Bone 40: 251-264, 2007.
8. Chambers TJ: Regulation of the differentiation and function of osteoclasts. J Pathol 192: 4-13, 2000.

9. Wada T, Nakashima T, Hiroshi N and Penninger JM: RANKL-RANK signaling in osteoclastogenesis and bone disease. Trends Mol Med 12: 17-25, 2006.
10. He Y, Staser K, Rhodes SD, Liu Y, Wu X, Park SJ, Yuan J, Yang X, Li X, Jiang L, *et al*: Erk1 positively regulates osteoclast differentiation and bone resorptive activity. PLoS One 6: e24780, 2011.
11. Yamamoto A, Miyazaki T, Kadono Y, Takayanagi H, Miura T, Nishina H, Katada T, Wakabayashi K, Oda H, Nakamura K and Tanaka S: Possible involvement of IkappaB kinase 2 and MKK7 in osteoclastogenesis induced by receptor activator of nuclear factor kappaB ligand. J Bone Miner Res 17: 612-621, 2002.
12. Matsumoto M, Sudo T, Saito T, Osada H and Tsujimoto M: Involvement of p38 mitogen-activated protein kinase signaling pathway in osteoclastogenesis mediated by receptor activator of NF-kappa B ligand (RANKL). J Biol Chem 275: 31155-31161, 2000.
13. Fu Y, Gu J, Wang Y, Yuan Y, Liu X, Bian J and Liu Z: Involvement of the mitogenactivated protein kinase signaling pathway in osteoprotegerininduced inhibition of osteoclast differentiation and maturation. Mol Med Rep 12: 6939-6945, 2015.
14. Boyle WJ, Simonet WS and Lacey DL: Osteoclast differentiation and activation. Nature 423: 337-342, 2003.
15. Asagiri M, Sato K, Usami T, Ochi S, Nishina H, Yoshida H, Morita I, Wagner EF, Mak TW, Serfling E and Takayanagi H: Autoamplification of NFATc1 expression determines its essential role in bone homeostasis. J Exp Med 202: 1261-1269, 2005.
16. Logar DB, Komadina R, Prezelj J, Ostanek B, Trost Z and Marc J: Expression of bone resorption genes in osteoarthritis and in osteoporosis. J Bone Miner Metab 25: 219-225, 2007.
17. Harvey AL: Natural products in drug discovery. Drug Discov Today 13: 894-901, 2008.
18. An J, Hao D, Zhang Q, Chen B, Zhang R, Wang Y and Yang H: Natural products for treatment of bone erosive diseases: The effects and mechanisms on inhibiting osteoclastogenesis and bone resorption. Int Immunopharmacol 36: 118-131, 2016.
19. He ZH, He MF, Ma SC and But PP: Anti-angiogenic effects of rhubarb and its anthraquinone derivatives. J Ethnopharmacol 121: 313-317, 2009.
20. Matsuda H, Tewtrakul S, Morikawa T and Yoshikawa M: Anti-allergic activity of stilbenes from Korean rhubarb (*Rheum undulatum* L.): Structure requirements for inhibition of antigen-induced degranulation and their effects on the release of TNF-alpha and IL-4 in RBL-2H3 cells. Bioorg Med Chem 12: 4871-4876, 2004.
21. Paneitz A and Westendorf J: Anthranoid contents of rhubarb (*Rheum undulatum* L.) and other Rheum species and their toxicological relevance. Eur Food Res Technol 210: 97-101, 1999.
22. Matsuda H, Morikawa T, Toguchida I, Park JY, Harima S and Yoshikawa M: Antioxidant constituents from rhubarb: Structural requirements of stilbenes for the activity and structures of two new anthraquinone glucosides. Bioorg Med Chem 9: 41-50, 2001.
23. Choi RJ, Chun J, Khan S and Kim YS: Desoxyrhapontigenin, a potent anti-inflammatory phytochemical, inhibits LPS-induced inflammatory responses via suppressing NF-κB and MAPK pathways in RAW 264.7 cells. Int Immunopharmacol 18: 182-190, 2014.
24. Choi SZ, Lee SO, Jang KU, Chung SH, Park SH, Kang HC, Yang EY, Cho HJ and Lee KR: Antidiabetic stilbene and anthraquinone derivatives from *Rheum undulatum*. Arch Pharm Res 28: 1027-1030, 2005.
25. Redlich K and Smolen JS: Inflammatory bone loss: Pathogenesis and therapeutic intervention. Nat Rev Drug Discov 11: 234-250, 2012.
26. Bradford MM: A rapid and sensitive method for the quantitation of microgram quantities of protein utilizing the principle of protein-dye binding. Anal Biochem 72: 248-254, 1976.
27. Livak KJ and Schmittgen TD: Analysis of relative gene expression data using real-time quantitative PCR and the 2(-delta deltaC(T)) method. Methods 25: 402-408, 2001.
28. Ngoc TM, Minh PT, Hung TM, Thuong PT, Lee I, Min BS and Bae K: Lipoxygenase inhibitory constituents from Rhubarb. Arch Pharm Res 31: 598-605, 2008.
29. Choi B, Kim S, Jang BG and Kim MJ: Piceatannol, a natural analogue of resveratrol, effectively reduced beta-amyloid levels via activation of alpha-secretase and matrix metalloproteinase-9. J Funct Foods 23: 124-134, 2016.
30. Pawlus AD, Sahli R, Bisson J, Rivière C, Delaunay JC, Richard T, Gomès E, Bordenave L, Waffo-Téguo P and Mérillon JM: Stilbenoid profiles of canes from vitis and muscandinia species. J Agric Food Chem 61: 501-511, 2013.
31. He X, Andersson G, Lindgren U and Li Y: Resveratrol prevents RANKL-induced osteoclast differentiation of murine osteoclast progenitor RAW 264.7 cells through inhibition of ROS production. Biochem Biophys Res Commun 401: 356-362, 2010.
32. Yamasaki T, Ariyoshi W, Okinaga T, Adachi Y, Hosokawa R, Mochizuki S, Sakurai K and Nishihara T: The dectin 1 agonist curdlan regulates osteoclastogenesis by inhibiting nuclear factor of activated T cells cytoplasmic 1 (NFATc1) through Syk kinase. J Biol Chem 289: 19191-19203, 2014.
33. Wilson SR, Peters C, Saftig P and Brömme D: Cathepsin K activity-dependent regulation of osteoclast actin ring formation and bone resorption. J Biol Chem 284: 2584-2592, 2009.
34. Shen T, Wang XN and Lou HX: Natural stilbenes: An overview. Nat Prod Rep 26: 916-935, 2009.
35. Chachay VS, Kirkpatrick CM, Hickman IJ, Ferguson M, Prins JB and Martin JH: Resveratrol-pills to replace a healthy diet? Br J Clin Pharmacol 72: 27-38, 2011.
36. Tou JC: Resveratrol supplementation affects bone acquisition and osteoporosis: Pre-clinical evidence toward translational diet therapy. Biochim Biophys Acta 1852: 1186-1194, 2015.
37. Kim JH and Kim N: Regulation of NFATc1 in osteoclast differentiation. J Bone Metab 21: 233-241, 2014.
38. Ikeda F, Nishimura R, Matsubara T, Tanaka S, Inoue J, Reddy SV, Hata K, Yamashita K, Hiraga T, Watanabe T, *et al*: Critical roles of c-Jun signaling in regulation of NFAT family and RANKL-regulated osteoclast differentiation. J Clin Invest 114: 475-484, 2004.
39. Böhm C, Hayer S, Kilian A, Zaiss MM, Finger S, Hess A, Engelke K, Kollias G, Krönke G, Zwerina J, *et al*: The alpha-isoform of p38 MAPK specifically regulates arthritic bone loss. J Immunol 183: 5938-5947, 2009.
40. Lee SE, Woo KM, Kim SY, Kim HM, Kwack K, Lee ZH and Kim HH: The phosphatidylinositol 3-kinase, p38, and extracellular signal-regulated kinase pathways are involved in osteoclast differentiation. Bone 30: 71-77, 2002.